Polymer Chemistry

Accepted Manuscript

ROYAL SOCIETY OF CHEMISTRY

www.rsc.org/polymers

Cite this: DOI: 10.1039/c0xx00000x

www.rsc.org/xxxxxx

ARTICLE TYPE

Synthesis and Properties of D-A Copolymers Based on Dithienopyrrole and Benzothiadiazole with Various Number of Thienyl Units as Spacer

Yanfang Geng,[a] Junzi Cong,[b] Keisuke Tajima,*[b] Qingdao Zeng[a] and Erjun Zhou*[a]

Received (in XXX, XXX) Xth XXXXXXXXX 20XX, Accepted Xth XXXXXXXXX 20XX

DOI: 10.1039/b000000x

Three kinds of donor-acceptor (D-A) type semiconducting copolymers in which electron donating unit of dithienopyrrole (DTP) and accepting unit of benzothiadiazole (BT) connected with different number of thienyl spacer (x = 0-2) were synthesized and used as electron donor materials in polymer solar cells (PSCs) combined with fullerene derivative. The optical band gaps of the polymers could be tuned from 1.41 eV to 1.61 eV by changing the number of the thiophene spacer. Electrochemical measurements showed that the increase of band gap is mainly due to the change of the lowest unoccupied molecular orbital (LUMO) energy level. The power conversion efficiency (PCE) of the polymer solar cells based on these three polymers and $PC_{70}BM$ reached 3.12% with x = 2 under the illumination of AM 1.5, 100 mW/cm^2 This approach could provide a simple strategy for designing high-performance D-A type photovoltaic polymers based on the existing polymers and a large potential to improve their performance further.

1 Introduction

Polymer solar cells (PSCs) have attracted much interest due to their great potential to be a renewable energy technology based on simple and low cost manufacture.[1-3] Concept of bulk heterojunction (BHJ) utilizing mixtures of a conjugated polymer and a fullerene derivative is regarded as the efficient system for the photovoltaic application.[4] The most representative active layer of the blend of regioregular poly(3-hexylthiophene) (P3HT) with fullerene derivatives were extensively investigated.[5-7] While the advantage of P3HT is its simple structure with relatively high hole mobility, the weak point of P3HT as the photovoltaic donor material towards the efficient PSCs is the mismatch of its absorption spectrum (absorption edge is about 650 nm) with the terrestrial solar spectrum. The band gap of P3HT (1.9 eV) is larger than the optimum band gap range (1.3-1.5 eV) for polymer-fullerene BHJ solar cells.[8] Hence, design of photovoltaic polymer with broader absorption toward longer wavelengths, especially in the near-infrared (NIR) range is necessary for high efficiency conjugated polymer donor materials.

Thanks to many attempts have been made to develop NIR absorbing polymers, notable improvement of the overall power-conversion efficiency (PCE) has been achieved.[9-11] One of the most powerful and flexible strategy to design low band gap conjugated polymers involves an alternating sequence of electron-donor (D) and electron-acceptor (A) moieties along the conjugated polymer main chain.[12, 13] The highest occupied molecular orbital (HOMO) and the lowest unoccupied molecular orbital (LUMO) of this so-called donor-acceptor (D-A) type copolymers are mainly localized on the donor and acceptor units, respectively, thus band gap can be well tuned by the choice of D and A. Such D-A strategy is now widely used as one of the most promising approaches to design efficient polymers for application to the polymer photovoltaic.

Thiophene is a simple and fundamental block to construct new D-A type copolymers. Recently, bridged dithiophene have attracted considerable attentions as donor unit because of its ability of fixing the dithiophene system into planar structure, which is much more efficient than the dithiophene in constructing highly-conjugated copolymers. Four bridging dithiophenes units with the atom of carbon (C), silicon (Si), germanium (Ge) and nitrogen (N) atom, afford cyclopenta[2,1-b;3,4-b']dithiophene (CPDT), dithienosilole (DTS), dithienogermole (DTG) and dithieno[3,2-*b*:2',3'-*d*]pyrrole (DTP), respectively.

CPDT was the first introduced into the low band gap polymers and the corresponding copolymer alternating CPDT with benzothiadiazole showed PCE of 5.5%, after using small amount of alkanedithiols to control the morphology of blend film.[14, 15] Later on, large amount of CPDT-based photovoltaic polymers were designed and synthesized.[16-20] In comparison with the C-C bond, longer C-Si bond shows less steric hindrance, which is directly resulted in the better π-π stacking along the conjugated polymer backbones.[21, 22] Polymers based on DTS normally have high hole mobility and strong light absorption in the visible region of the solar spectrum and hence the improvement in

[a] *National Center for Nanoscience and Technology, No. 11 Beiyitiao, Zhongguancun, Beijing 100190, P. R. China. E-mail: zhouej@nanoctr.cn*

[b] *Emergent Functional Polymers Research Team, RIKEN Center for Emergent Matter Science (CEMS), 2-1 Hirosawa, Wako 351-0198, Japan. E-mail: keisuke.tajima@riken.jp*

† Electronic Supplementary Information (ESI) available: [XRD patterns, DFT and TD-DFT calculations]. See DOI: 10.1039/b000000x/

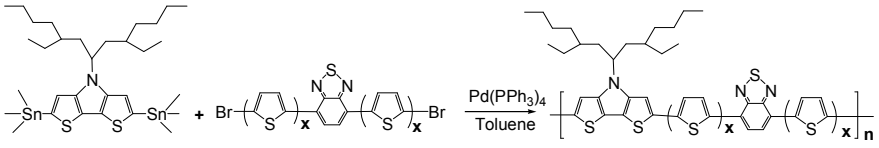

1

M0 (x=0)
M1 (x=1)
M2 (x=2)

PDTP-BT (x=0)
PDTP-DTBT (x=1)
PDTP-DT2BT (x=2)

Scheme 1. Synthetic route of three dithienopyrrole-based donor-acceptor type copolymers with thienyl spacers.

photovoltaic performance, which reached 5.1%.[12] DTG show lower intermolecular steric hindrance than DTS because of longer C-Ge bond compared to the C-Si, resulting in the corresponding DTG-containing solar cells exhibit higher short-current and fill factor.[23-25] Planar dithieno[3,2-b:2',3'-d]pyrrole (DTP), with good π-conjugation, showed great potential for use in organic electronic materials.[26] D-A type photovoltaic polymers with DTP as electron-donating unit, exhibiting low band gap and enhanced solubility, have been intensively applied to PSCs.[27, 28] In our previous study, the PSCs based on DTP-containing copolymer and $PC_{70}BM$ showed short-circuit current as high as 22.6 mA/cm,[29] indicating that DTP-containing copolymers could be as a promising building block for superior photovoltaic performance.

On the other hand, benzothiadiazole (BT) containing the electron-withdrawing imine (-C=N-) nitrogen has been widely used as a strong acceptor in D-A copolymers.[30, 31] Numerous attempts to develop novel D-A copolymers have shown that the 4,7-dithien-2-yl-2,1,3-benzothiadiazole (DTBT) is an effective acceptor unit, and the photovoltaic devices made from blends with fullerene derivatives show PCE up to 5.4%.[14, 32-36] In 2008, we reported the synthesis of a copolymer between the DTP donor and DTBT acceptor.[27] It has been proved that the thienyl ring can enhance the π-π stacking intermolecular interactions and led to high charge carrier mobility.[37] In addition, the ordered structure can enhance the carrier mobility, thereby symmetric thienyl units along the polymer main chain are selected. In these regards, it might be a simple and effective method to tune the properties of D-A type photovoltaic polymers through introduce thienyl group as spacer between donor and acceptor segments in the backbone.

In this study, three kinds of low band gap copolymers integrating DTP as donor block and the most-used BT as acceptor unit with was synthesized. Different number of thienyl (T) as spacer was introduced along the copolymer main chain to investigate the effect on the optical, electrochemical and photovoltaic performance. [6,6]-Phenyl-C_{71}-butyric acid methyl ester ($PC_{70}BM$) was used as acceptor in the blended film of copolymers:$PC_{70}BM$. Different solvents (chlorobenzene (CB) and 1,2-dichlorobenzene (DCB)) were tested to build an optimized interpenetrated network in the active film, and the corresponding film properties and the photovoltaic devices performance are discussed in detail.

2 Results and Discussions

2.1 Material Synthesis

To obtain these three designed copolymers a Stille reaction was employed as shown in Scheme 1. Subsequently, three polymers

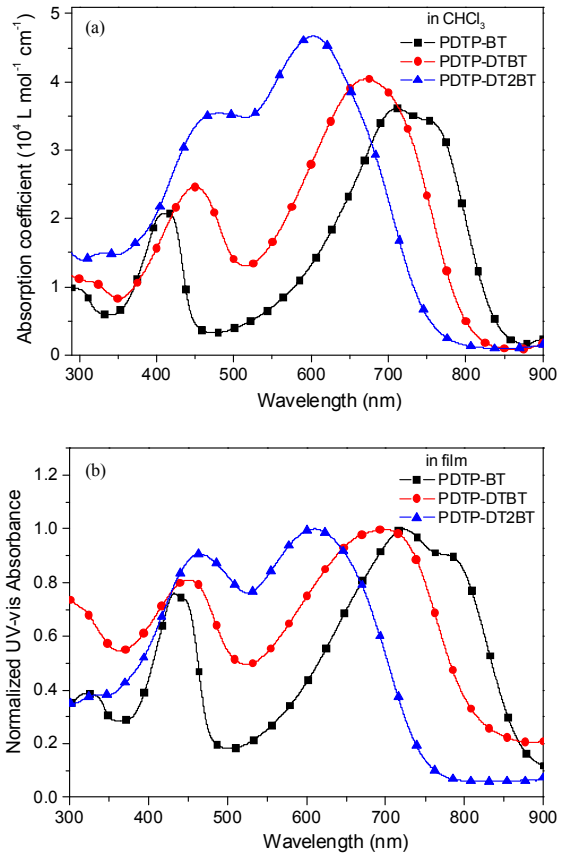

Figure 1. UV-vis absorption spectra of PDTP-BT, PDTP-DTBT and PDTP-DT2BT three polymers (a) in $CHCl_3$ solution and (b) in film on a quartz plate.

PDTP-BT, PDTP-DTBT, PDTP-DT2BT were synthesized by coupling between 2,6-di(trimethyltin)-N-[2'-ethylhexyl]-3-ethylheptanyla-dithieno[3,2-b:2',3'-d]pyrrole () and 4,7-dibromo-2,1,3-benzothiadiazole (**M0**), 4,7-di(2'-bromothien-5'-yl)-2,1,3-benzothiadiazole (**M1**) and 4,7-di(2,2'-bromothien-5'-yl)-2,1,3-benzothiadiazole (**M2**) with tetrakis(triphenylphosphine)palladium(0) as catalyst in the yields of 55%, 65% and 82%, respectively. The chemical structures of these copolymers were verified by ^1H NMR spectroscopy. All of these copolymers are soluble in common organic solvents such as $CHCl_3$, CB and DCB due to the branched-chain substituent on the DTP moiety.

2.2 Optical Properties

Table 1: The optical and electrochemical properties of three polymers.

Polymers	Mw (kg/mol)	PDI	UV-vis absorption spectra			Cyclic voltammetry		
			Solution	Film	E_g^{opt} (eV)	*p*-doping	*n*-doping	E_g^{ec} (eV)
			λ_{max} (nm)	λ_{max} (nm)		φ_{ox} / HOMO (V) / (eV)	φ_{red} / LUMO (V) / (eV)	
PDTP-BT	16.3	2.8	413 / 711	433 / 723	1.41	0.18 / −4.98	−1.29 / −3.51	1.47
PDTP-DTBT	6.0	3.4	450 / 671	451 / 697	1.46	0.20 / −5.00	−1.37 / −3.43	1.57
PDTP-DT2BT	21.2	2.3	480 / 603	464 / 611	1.61	0.19 / −4.99	−1.40 / −3.40	1.60

Figure 1 shows the optical absorption spectra of PDTP-BT, PDTP-DTBT and PDTP-DT2BT in $CHCl_3$ solutions and in thin films spin-coated on quartz plate. The absorption maximum

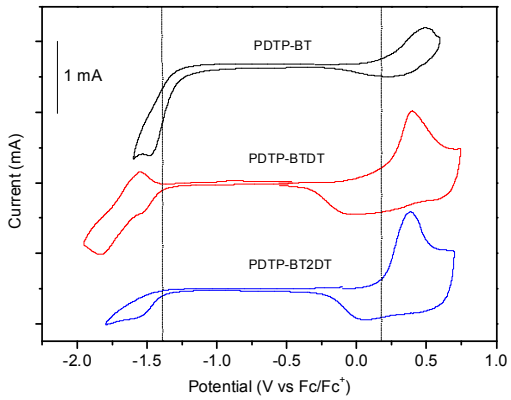

Figure 2. Cyclic voltammograms of the polymers films deposited on a platinum plate (~1 cm^2) in an acetonitrile solution of 0.1 M $[Bu_4N]PF_6$ (Bu = butyl) at a scan rate of 50 mV/s.

wavelength in the solutions and the films and the optical band gap deduced from the absorption onsets are summarized in Table 1. Judging from the splitting of the absorption bands, it can be speculated that the polymers have typical absorption characteristics of D-A type copolymers with the π-π* and charge transfer-type transitions.

Comparing the polymers PDTP-BT and PDTP-DT2BT with previously synthesized polymers PDTP-DTBT,[27] the difference in their absorption is distinct. PDTP-DTBT solution showed two prominent absorption maxima at 450 and 671 nm, while PDTP-BT and PDTP-DT2BT solution demonstrates two main absorption maxima at 413 and 711 nm and at 480 and 603 nm, respectively. Although the absorption peaks in long wavelength blue-shifted by 40 nm and 108 nm with insert one and two thienyl spacer to PDTP-BT, but the absorption coefficient at the absorption maxima increase from 3.6×10^4 (PDTP-BT) to 4.0×10^4 (PDTP-DTBT) and 4.7×10^4 L mol^{-1} cm^{-1} (PDTP-DT2BT), respectively.

In thin films, these three copolymers exhibit similar shapes and red-shifted absorption spectra compared with those in the solutions, which indicate stronger intermolecular interactions in the solid state.[38] In addition, PDTP-BT film shows a large shoulder peak at 800 nm, while no shoulder peaks was observed for PDTP-DTBT and PDTP-DT2BT, indicating that stronger intermolecular interaction in PDTP-BT than the others. These results suggest that the absorption of the polymers, both absorption peaks and absorption coefficient could be readily controlled by tailoring the number of thienyl spacer along the polymers.[37, 39, 40]

The absorption edge shifts from ca. 900 nm in PDTP-BT to ca. 850 nm in PDTP-DTBT and ca. 750 nm in PDTP-DT2BT, reflecting the broadening of the optical band-gap in sequence. Table 1 shows the optical band-gaps (E_g^{opt}) of all polymers estimated from the corresponding UV-vis absorption onset. PDTP-DT2BT, PDTP-DTBT and PDTP-BT have optical band gaps of 1.61, 1.46 and 1.41 eV, respectively, which are close to the ideal value of 1.5 eV for PSC application.

These changes of the absorption spectra upon the introduction of thienyl groups can be qualitatively understood from density functional theory (DFT) calculations of the corresponding model compounds (Figure S1). The optimized structures show that all the polymer backbones are mostly planar. Time dependent DFT calculations show that the absorption band in the longer wavelength is mainly attributed to the transition from HOMO delocalized in D-A backbone to LUMO localized in DTP units for all the polymers. On the other hand, the absorption in the shorter wavelength is largely contributed from transition from HOMO to LUMO+1, which is similar to π-π* transition in polythiophene judging by the shape of the orbitals. Therefore, the introduction of more thienyl spacer could stabilize LUMO+1 (π*) due to the better conjugation, resulting in the red-shift of the absorption band. At the same time, it could decrease the D-A nature of the polymer due to the weaken electron acceptability of DTP, resulting in the blue-shift of the charge transfer bands.

2.3 Electrochemical Properties

Electrochemical cyclic voltammetry has been widely employed to investigate the electrochemical behavior of the polymers and estimate the HOMO and the LUMO energy level of the conjugated polymers. Representative cyclic voltammogram (CV) curves of these copolymers are shown in Figure 2, while the obtained HOMO and LUMO values are summarized in Table 1. The onset reduction potential (φ_{red}) of PDTP-BT is −1.29 V *vs.* Fc/Fc^+, while the onset oxidation potential (φ_{ox}) is +0.18 V *vs.* Fc/Fc^+. From the values of reduction potential and oxidation potential, the LUMO and HOMO energy level of PDTP-BT were calculated to be −3.51 and −4.98 eV, according to the equations of LUMO = $-e(\varphi_{red} + 4.8)$ (eV) and HOMO = $-e(\varphi_{ox} + 4.8)$ (eV). The LUMO and HOMO energy levels of PDTP-DTBT and PDTP-DT2BT were estimated through the similar method to be −3.43, −3.40 eV and −5.00, −4.99 eV, respectively. These results

indicate that changing the number of thienyl spacer along the conjugated copolymers have obvious effect on the LUMO energy level. The electrochemical band-gaps (E_g^{EC}) of all polymers are in accordance with the results of E_g^{opt}.

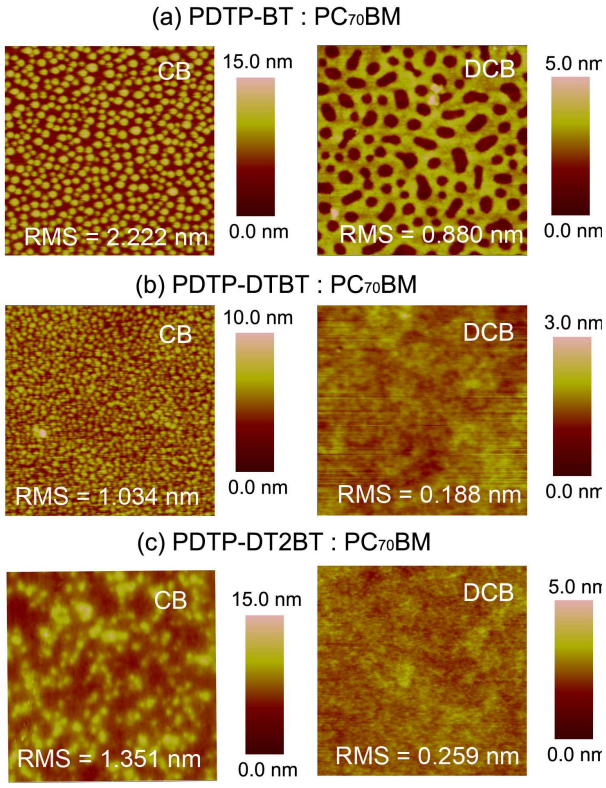

Figure 3. AFM height images of the mixed films with $PC_{70}BM$ and (a) PDTP-BT, (b) PDTP-DTBT and (c) PDTP-DT2BT spin-coated from different solutions (CB and DCB)

2.4 Microstructure

Crystalline order of the copolymer thin films was investigated by X-ray diffraction (XRD) scans (Figure S2). In the out-of-plane measurement, the XRD pattern of PDTP-BT reveals a weak peak near 6°, and there is no clear peak for PDTP-DTBT and PDTP-DT2BT, suggesting that they exhibit amorphous structures in film, which might be due to the bulky side chain in DTP building block. Change in the number of thienyl spacer in this system does not significantly affect the aggregation behaviour of the polymer main chains.

The microstructure of blend films of the copolymers with fullerene derivatives is known to have large effect on the charge transport properties and the corresponding efficiencies of PSCs. Here, the atomic force microscopy (AFM) was applied to investigate the morphology of the blend film of the polymer:$PC_{70}BM$ fabricated from CB and DCB solutions, respectively, as shown in Figure 3. For PDTP-BT:$PC_{70}BM$, both CB and DCB gave the films with obvious phase separation with a room mean square (RMS) of 2.222 nm and 0.880 nm, respectively, which might be due to the poor miscibility of two materials. For PDTP-DTBT and PDTP-DT2BT, the blend film of polymer/$PC_{70}BM$ spin-coated from CB were also rough, but the blend films fabricated from DCB displayed a much smoother surface with a RMS of 0.188 nm and 0.259nm, respectively. This

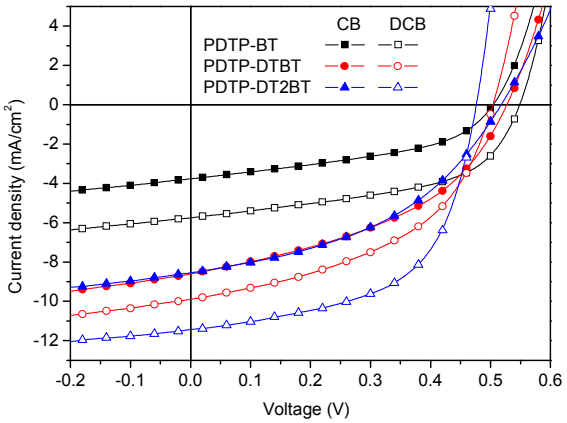

Figure 4. *J-V* curves of the polymer solar cells based on PDTP-BT, PDTP-DTBT and PDTP-DT2BT under the illumination of AM 1.5, 100 mW/cm^2.

smaller roughness of the blend films indicates that the domain size of the phase separation of the donor-acceptor interpenetrating network could be reduced, which could be beneficial for the exciton charge separation and charge transport. These results indicate that the morphologies of these polymers with $PC_{70}BM$ are quite sensitive to the solvents used for device processing and the introduction of thienyl spacer could improve the miscibility.

2.5 Photovoltaic Properties

The photovoltaic properties of these three copolymers PDTP-BT, PDTP-DTBT and PDTP-DT2BT were studied by fabricating bulk heterojunction BHJ-type PSCs with a conventional sandwich configuration of ITO/PEDOT:PSS/Polymer:$PC_{70}BM$/Ca/Al. The effective areas of the PSCs, contributing to photocurrent, were defined using a metal photomask during irradiation with simulated solar light. The devices were optimized by changing many factors, such as the ratio of the donor and the acceptor, the thickness of blend films and the cathode metal. The best performance was obtained with the thickness of the active layer of 80-90 nm, the copolymers:$PC_{70}BM$ ratio of 1:2 (by weight) and the Ca/Al used as the cathode.

Figure 4 shows the *J-V* curves of the optimized PSCs based on three polymers under illumination of AM 1.5 simulated solar light (100 mW/cm^2). The PSCs with two kinds of solvents CB and DCB for the spin-coting of the active layers were investigated, and the corresponding photovoltaic parameters of the devices open-circuit voltage (V_{OC}), short-circuit current density (J_{SC}), fill factor (*FF*) and PCE are summarized in Table 2. When CB was used as the solvent, all the combinations showed a relatively low PCE of 0.87%, 1.97% and 1.92% in the devices with PDTP-BT:$PC_{70}BM$, PDTP-DTBT:$PC_{70}BM$ and PDTP-DT2BT:$PC_{70}BM$ respectively. DCB solvent induced high performance photovoltaic devices due to the optimized interpenetrated network of the active film. The best devices of PDTP-BT and PDTP-DTBT shows PCE of 1.64% and 2.37%, respectivley. The polymer PDTP-DT2BT exhibits the highest PCE of 3.12%, ascribed to the largest of J_{SC} = 11.43 mA/cm^2 with slightly lower V_{OC} of 0.54 V and slightly higher FF of 0.57 than the other polymers. The V_{OC} values of the devices are around 0.5 V, suggesting the addition of the thienyl units do not affect the

Table 2. Device characteristics of PSCs based on the DTP and BT based copolymers in combination with $PC_{70}BM$.

Polymer : Acceptor (wt/wt)	Solvent	V_{OC} (V)	J_{SC} (mA/cm^2)	FF	PCE
PDTP-BT : $PC_{70}BM$ (1:2)	CB	0.50	3.77	0.45	0.87%
	DCB	0.54	5.75	0.53	1.64%
PDTP-DTBT : $PC_{70}BM$ (1:2)	CB	0.52	8.61	0.44	1.97%
	DCB	0.50	9.90	0.48	2.37%
PDTP-DT2BT : $PC_{70}BM$ (1:2)	CB	0.52	8.55	0.43	1.92%
	DCB	0.48	11.43	0.57	3.12%

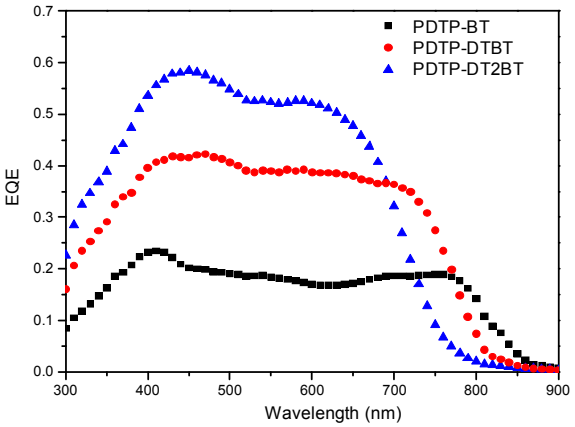

Figure 5. EQE curves of the polymer solar cells based on PDTP-BT, PDTP-DTBT and PDTP-DT2BT under the illumination of AM 1.5, 100 mW/cm^2.

main chain distortion. This coincide well with the similar HOMO energy levels for the copolymers measured by CV. These results indicate that the PCEs of the photovoltaic devices based on PDTP-DT2BT:$PC_{70}BM$ were higher than those of PDTP-DTBT:$PC_{70}BM$ and PDTP-BT:$PC_{70}BM$. Overall, it is an effective approach to improve the photovoltaic performance of PDTP-based copolymers by increasing the number of unsubstituted thienyl units along the copolymers backbone.

Figure 5 shows the external quantum efficiency (EQE) plots of the devices based on three copolymer:$PC_{70}BM$ combinations under the illumination of monochromatic light. With the increase of thienyl spacer, the EQE response wavelengths show blue shift, similar tendency with the absorption spectra, but the EQE peak values was higher in PDTP-DT2BT (58%) compared to PDTP-BT (23%) or PDTP-DTBT (42%) . The shapes of the EQE curves of the devices in the range of 450-700 nm could be assigned to the stronger absorption of $PC_{70}BM$.

3 Conclusions

In conclusion, three low band gap D-A copolymers, based on DTP donor and BT acceptor, with different number of thienyl spacer along the backbone have been designed and synthesized. The thienyl spacer makes the absorption spectra peak blue-shift at the longer wavelength range, and red-shift at the low wavelength range. Under 1.5 G 100 mW/cm^2 illumination, a best PCE of 3.12% for PDTP-DT2BT was recorded, with a V_{OC} = 0.48 V, a J_{SC} = 11.43 mA/cm^2, and a FF = 0.57. Although the best PCE is still not high enough for the commercial use, our optimization by designing suitable molecule structure, selecting different solvents as well as changing other factors could provide useful information for further studies of the commercialized PSCs.

4 Experimental Section

4.1 Materials

All the chemicals were purchased from Alfa, Aldrich or Wako and used without further purification. The following compounds were synthesized according to the procedure in the literature: 2,6-di(trimethyltin)-N-[2'-ethylhexyl]-3-ethylheptanyla-dithieno[3,2-b:2',3'-d]pyrrole (**1**) and 4,7-di(2,2'-bithien-5-yl)- 2,1,3-benzothiadiazole (**M2**).[27]

4.2 Synthesis of Polymers

These three polymers were synthesized by a similar procedure as the synthesis of PDTP-DTBT (M_w= 6.0 kg/mol; polydispersity index (PDI) = 3.4) in our previous report. [27] For PDTP-BT, the detailed synthetic process is as follows. **1** (0.56 mmol, 416 mg), **M0** (0.56 mmol, 165 mg), and dry toluene (15 mL) were added to a 50 mL double-neck round bottom flask. The reaction container was purged with N_2 for 30 min to remove O_2. $Pd(PPh_3)_4$ (5%, 32 mg) was added, and heated up to 110 °C. The solution was stirred at 110 °C for 48 h. The dark blue sticky solution was cooled down to room temperature and poured into methanol (200 mL), and the dark green precipitates were collected by filtration, and then washed with methanol. The solid was dissolved in $CHCl_3$ (150 mL) and passed through a column packed with alumina, celite, and silica gel. The column was eluted with $CHCl_3$. The combined polymer solution was concentrated to 30 mL and was poured into methanol (300 mL). After which, the precipitates were collected and dried (170 mg, 55%). ^{1}H NMR ($CDCl_3$, 400MHz): δ(ppm): 8.0-7.1 (m, 4H), 4.5 (br, 1H), 2.1-0.5 (m, 34H). M_w= 16.3 kg/mol; PDI = 2.80.

The similar synthetic route for PDTP-DT2BT is also shown in Scheme 1, starting with **1** (0.53 mmol, 394 mg), **M2** (0.53 mmol, 330 mg), dry toluene (15 mL) and $Pd(PPh_3)_4$ (5%, 31 mg). Yield: 380 mg (82%).^{1}H NMR ($CDCl_3$, 400MHz): δ(ppm): 8.0-6.1 (m, 4H), 4. 4 (br, 1H), 2.0-0.6 (m, 34H). M_w= 21.2 kg/mol; PDI = 2.30.

4.3 Characterization

^{1}H NMR (400 MHz) spectra were measured using a JEOL Alpha FT-NMR spectrometer equipped with an Oxford superconducting magnet system at 400 MHz in deuterated

chloroform solution with TMS as reference. Gel permeation chromatography (GPC) was performed on a Shimadzu Prominence system equipped with a UV detectorusing $CHCl_3$ containing triethylamine as the eluent. Absorption spectra were measured using a SHIMADZU spectrophotometer MPC-3100. Cyclic voltammograms (CVs) were recorded on an HSV-100 (Hokuto Denkou) potentiostat. A Pt plate coated with a thin polymer film was used as the working electrode. A Pt wire and an Ag/Ag+ (0.01 M of $AgNO_3$ in acetonitrile) electrode were used as the counter and the reference electrodes (calibrated vs. Fc/Fc^+), respectively. AFM measurement was carried out using a Digital Instrumental Nanoscope 31 operated in the tapping mode. Out-of-plane and in-plane XRD scans of polymer thin films on silicon wafers substrates were performed on a Smartlab X-ray diffractometer (Rigaku) using monochromatized Cu Kα radiation ($\lambda = 0.154$ nm) generated at 45 kV and 200 mA.

4.4 Fabrication and Characterization of Polymer Solar Cells

PSCs were constructed in the traditional sandwich structure through several steps. ITO-coated glass substrates were cleaned by ultrasonication sequentially in detergent, water, acetone, and 2-propanol. After drying the substrate, PEDOT:PSS (Baytron P) was spin-coated (4000 rpm for 30 s) on ITO. The film was dried at 140 °C under N_2 atmosphere for 30 min. After cooling the substrate, a chlorobenzene solution of the PDTP-DTBT and $PC_{70}BM$ mixture (1:2, by weight) was spin-coated. The PDTP-DTBT concentration was 10 mg/mL. Ca and Al electrodes were then successively evaporated under high vacuum (approximately 2×10^{-4} Pa) in the ULVAC UPC-260F vacuum evaporation system. The thickness of the Ca electrode was 20 nm, and that of Al electrode was 60 nm. The current–voltage characteristics of the solar cells were measured using the Agilent Technologies E5273A C-V measurement system. PCE was examined using a xenon-lamp-based solar simulator (Peccell Technologies PCE-L11). Light intensity was adjusted by a standard silicon solar cell with an optical filter (Bunkou Keiki BS520).

Acknowledgements

We acknowledge financial support from the New Energy and Industrial Technology Development Organization (NEDO), Japan. The author also thanks the support from the National Natural Science Foundation (No. 51203030).

Notes and references

1. C. J. Brabec, N. S. Sariciftci and J. C. Hummelen, *Adv. Func. Mater.*, 2001, **11**, 15-26.
2. D. Mühlbacher, M. Scharber, M. Morana, Z. Zhu, D. Waller, R. Gaudiana and C. Brabec, *Adv. Mater.*, 2006, **18**, 2884-2889.
3. K. M. Coakley and M. D. McGehee, *Chem. Mater.*, 2004, **16**, 4533-4542.
4. G. Yu, J. Gao, J. C. Hummelen, F. Wudl and A. J. Heeger, *Science*, 1995, **270**, 1789-1791.
5. S. E. Shaheen, C. J. Brabec, N. S. Sariciftci, F. Padinger, T. Fromherz and J. C. Hummelen, *Appl. Phys. Lett.*, 2001, **78**, 841-843.
6. P. W. M. Blom, V. D. Mihailetchi, L. J. A. Koster and D. E. Markov, *Adv. Mater.*, 2007, **19**, 1551-1566.
7. J. G. Labram, J. Kirkpatrick, D. D. C. Bradley and T. D. Anthopoulos, *Adv. Energy Mater.*, 2011, **1**, 1176-1183.
8. M. C. Scharber, D. Mühlbacher, M. Koppe, P. Denk, C. Waldauf, A. J. Heeger and C. J. Brabec, *Adv. Mater.*, 2006, **18**, 789-794.
9. J. Hou, Z. a. Tan, Y. Yan, Y. He, C. Yang and Y. Li, *J. Am. Chem. Soc.*, 2006, **128**, 4911-4916.
10. Y. Li and Y. Zou, *Adv. Mater.*, 2008, **20**, 2952-2958.
11. Y. Liang, D. Feng, Y. Wu, S. T. Tsai, G. Li, C. Ray and L. Yu, *J. Am. Chem. Soc.*, 2009, **131**, 7792-7799.
12. J. Hou, H. Y. Chen, S. Zhang, G. Li and Y. Yang, *J. Am. Chem. Soc.*, 2008, **130**, 16144-16145.
13. H. Y. Chen, J. Hou, S. Zhang, Y. Liang, G. Yang, Y. Yang, L. Yu, Y. Wu and G. Li, *Nat. Photon.*, 2009, **3**, 649-653.
14. M. Svensson, F. Zhang, S. C. Veenstra, W. J. H. Verhees, J. C. Hummelen, J. M. Kroon, O. Inganäs and M. R. Andersson, *Adv. Mater.*, 2003, **15**, 988-991.
15. J. Peet, J. Y. Kim, N. E. Coates, W. L. Ma, D. Moses, A. J. Heeger and G. C. Bazan, *Nat. Mater.*, 2007, **6**, 497-500.
16. J. C. Bijleveld, M. Shahid, J. Gilot, M. M. Wienk and R. A. J. Janssen, *Adv. Func. Mater.*, 2009, **19**, 3262-3270.
17. Z. Li, S. W. Tsang, X. M. Du, L. Scoles, G. Robertson, Y. G. Zhang, F. Toll, Y. Tao, J. P. Lu and J. F. Ding, *Adv. Func. Mater.*, 2011, **21**, 3331-3336.
18. Y. J. Cheng, Y. J. Ho, C. H. Chen, W. S. Kao, C. E. Wu, S. L. Hsu and C. S. Hsu, *Macromolecules*, 2012, **45**, 2690-2698.
19. S. Das, P. B. Pati and S. S. Zade, *Macromolecules*, 2012, **45**, 5410-5417.
20. C. Y. Chang, L. Zuo, H. L. Yip, Y. Li, C. Z. Li, C. S. Hsu, Y. J. Cheng, H. Chen and A. K. Y. Jen, *Adv. Func. Mater.*, 2013, **23**, 5084-5090.
21. M. C. Scharber, M. Koppe, J. Gao, F. Cordella, M. A. Loi, P. Denk, M. Morana, H. J. Egelhaaf, K. Forberich, G. Dennler, R. Gaudiana, D. Waller, Z. Zhu, X. Shi and C. J. Brabec, *Adv. Mater.*, 2010, **22**, 367-370.
22. H. Y. Chen, J. Hou, A. E. Hayden, H. Yang, K. N. Houk and Y. Yang, *Adv. Mater.*, 2010, **22**, 371-375.
23. T. Y. Chu, J. Lu, S. Beaupré, Y. Zhang, J. R. Pouliot, S. Wakim, J. Zhou, M. Leclerc, Z. Li, J. Ding and Y. Tao, *J. Am. Chem. Soc.*, 2011, **133**, 4250-4253.
24. C. M. Amb, S. Chen, K. R. Graham, J. Subbiah, C. E. Small, F. So and J. R. Reynolds, *J. Am. Chem. Soc.*, 2011, **133**, 10062-10065.
25. Z. P. Fei, J. S. Kim, J. Smith, E. B. Domingo, T. D. Anthopoulos, N. Stingelin, S. E. Watkins, J. S. Kim and M. Heeney, *J. Mater. Chem.*, 2011, **21**, 16257-16263.
26. J. Y. Liu, R. Zhang, G. Sauve, T. Kowalewski and R. D. McCullough, *J. Am. Chem. Soc.*, 2008, **130**, 13167-13176.
27. E. Zhou, M. Nakamura, T. Nishizawa, Y. Zhang, Q. Wei, K. Tajima, C. Yang and K. Hashimoto, *Macromolecules*, 2008, **41**, 8302-8305.
28. E. Zhou, S. Yamakawa, K. Tajima, C. Yang and K. Hashimoto, *Chem. Mater.*, 2009, **21**, 4055-4061.
29. E. Zhou, J. Cong, K. Hashimoto and K. Tajima, *Energy Environ. Sci.*, 2012, **5**, 9756-9759.
30. H. Zhou, L. Yang, S. C. Price, K. J. Knight and W. You, *Angew. Chem. Int. Ed.*, 2010, **49**, 7992-7995.
31. K. H. Ong, S. L. Lim, H. S. Tan, H. K. Wong, J. Li, Z. Ma, L. C. H. Moh, S. H. Lim, J. C. de Mello and Z. K. Chen, *Adv. Mater.*, 2011, **23**, 1409-1413.
32. L. H. Slooff, S. C. Veenstra, J. M. Kroon, D. J. D. Moet, J. Sweelssen and M. M. Koetse, *Appl. Phys. Lett.*, 2007, **90**, 143506.
33. P. L. T. Boudreault, A. Michaud and M. Leclerc, *Macromol. Rapid Comm.*, 2007, **28**, 2176-2179.
34. E. Wang, L. Wang, L. Lan, C. Luo, W. Zhuang, J. Peng and Y. Cao, *Appl. Phys. Lett.*, 2008, **92**, 033307.
35. N. Blouin, A. Michaud and M. Leclerc, *Adv. Mater.*, 2007, **19**, 2295-2300.
36. L. Liao, L. Dai, A. Smith, M. Durstock, J. Lu, J. Ding and Y. Tao, *Macromolecules*, 2007, **40**, 9406-9412.
37. M. Zhang, X. Guo, Z. G. Zhang and Y. Li, *Polymer*, 2011, **52**, 5464-5470.
38. G. Li, V. Shrotriya, J. Huang, Y. Yao, T. Moriarty, K. Emery and Y. Yang, *Nat. Mater.*, 2005, **4**, 864-868.
39. M. J. Zhang, X. Guo and Y. F. Li, *Macromolecules*, 2011, **44**, 8798-8804.
40. P. M. Beaujuge, W. Pisula, H. N. Tsao, S. Ellinger, K. Müllen and J. R. Reynolds, *J. Am. Chem. Soc.*, 2009, **131**, 7514-7515.